ROYAL SOCIETY
OF CHEMISTRY

PAPER

Polyoxazoline functionalized magnetic spinel iron oxide nanoparticles for efficient removal of pharmaceuticals and heavy metal ions from water

Agnese Ricci,*[a] Luca Stefanuto, [ID] [a] Sara Del Galdo, [ID] [a] Simone Pepi,[b] Valerio Graziani,[c] Stefano Casciardi,[d] Sawssen Slimani,[e,f] Gaspare Varvaro,[e] Davide Peddis, [ID] [e,f] Luca Tortora, [ID] [a,c] Barbara Capone, [ID] [a] Claudio Rossi,[b] Daniela Tofani,[a] Giancarlo Masci [ID] *[g] and Tecla Gasperi [ID] *[a,h]

This study introduces a novel class of multifunctional hybrid materials for advanced water remediation, based on Fe_3O_4 superparamagnetic nanoparticles functionalised with tailored polyoxazoline coatings (PiPOx and PAmOx). These materials uniquely combine the high selective adsorption capacity of the polymer coating – engineered to target both organic pollutants and heavy metal ions – with the inherent magnetic responsiveness of the Fe_3O_4 core, enabling efficient contaminant removal and facile particle recovery under an external magnetic field. Detailed adsorption experiments reveal striking differences in performances between the two hybrid nanoparticles. Fe_3O_4@PAmOx exhibits exceptional efficacy in removing organic pollutants from aqueous solutions, achieving recovery rates exceeding 80% $\pm$ 2 for a range of tested contaminants. Conversely, Fe_3O_4@PiPOx demonstrates a pronounced affinity for heavy metal ions, particularly Pb^{2+}, with a recovery rate surpassing 25% $\pm$ 2. This selective adsorption behavior indicates that Fe_3O_4@PAmOx is optimally suited for the remediation of organic pollutants, whereas Fe_3O_4@PiPOx proves more effective in addressing heavy metal contamination. The synergistic combination of Fe_3O_4@PiPOx and Fe_3O_4@PAmOx offers a versatile and highly efficient solution for wastewater treatment capitalizing on their dual capabilities to selectively adsorb pharmaceutical residues and heavy metal ions, while preserving their magnetic properties following surface functionalization. This approach underscores the significant potential of these hybrid systems in practical water purification applications, facilitating the effective targeting of both organic and inorganic contaminants and providing a viable path towards sustainable water management.

[a]*Department of Science, Roma Tre University, via della Vasca Navale 79, 00146 Rome, Italy. E-mail: Tecla.Gasperi@uniroma3.it, Agnese.Ricci@uniroma3.it*
[b]*Department of Biotechnology, Chemistry and Pharmacy, University of Siena, Via Aldo Moro 2, 53100 Siena, Italy*
[c]*National Institute for Nuclear Physics (INFN), Tre via della Vasca Navale 84, Rome, 00146, Italy*
[d]*Department of Occupational Hygiene, INAIL, Via di Fontana Candida 1, 00078 Monte Porzio Catone, Italy*
[e]*Institute of Structure of Matter, National Research Council (CNR), Nanostructured Magnetic Materials Laboratory (nM2-Lab), Via Salaria Km 29.300, 00015 Monterotondo Scalo, RM, Italy*
[f]*Department of Chemistry and Industrial Chemistry (DCIC), University of Genova, Nanostructured Magnetic Materials Laboratory (nM2-Lab), Via Dodecaneso 31 16146, Genova, Italy*
[g]*Department of Chemistry, Sapienza University, Piazzale A. Moro 5, 00185 Rome, Italy. E-mail: Giancarlo.Masci@uniroma1.it*
[h]*Laboratory of Nanomaterials for Environment and Health (NAMES), Biostructures and Biosystems National Institute (INBB), Via dei Carpegna 19, 00165 Rome, Italy*

Introduction

In recent years, the escalating contamination of water bodies by pharmaceutical compounds and heavy metal pollutants poses a significant and multifaceted environmental threat, demanding innovative remediation strategies.[2,3] Heavy metals, including lead, cadmium, cobalt, chromium, and zinc are particularly hazardous due to their toxicity, persistence in the environment, and potential to bioaccumulate in living organisms.[4–7] Indeed, these toxic metals are listed among the top 20 most dangerous substances by the U.S. Environmental Protection Agency and the Agency for Toxic Substances and Disease Registry. Human exposure occurs through various pathways, including dermal contact, inhalation, and ingestion of contaminated water. Once absorbed, these metal ions interact with biomolecules, forming harmful compounds that are difficult to eliminate. In fact, upon absorption, metal ions disrupt biological systems through toxico-dynamic mechanisms, such as protein denaturation, oxidative

stress caused by reactive oxygen species (ROS), and DNA damage. This leads to impaired cellular function and mutations.[1,8] Their accumulation in vital organs (liver, kidneys, heart, and brain) can impair normal physiological processes, leading to organ damage, systemic failures, and diverse clinical manifestations such as headaches, nausea, vomiting, and cardiovascular diseases. For instance, cadmium's oral LD_{50} is 5.2 mg kg^{-1}, with chronic exposure linked to neurological damage, kidney disease, and cancer in humans.[1,9,10] An additional challenge in water remediation is the presence of pharmaceuticals and their metabolites in the aquatic environment.[11–14] Continuous discharge of pharmaceuticals into water bodies exert significant toxic effects on aquatic life, even at concentrations as low as nanograms per liter (ng L^{-1}). The slow degradation rates of many pharmaceuticals, coupled with ongoing emissions and the inefficiency of current wastewater treatment processes, result in steadily increasing concentrations. The EPA/WHO's regulatory limits for different organic compounds highlight the high toxicity and persistence of pharmaceutical pollutants, as well as the need for effective removal technologies.[15,16] Over 150 active pharmaceutical compounds have been detected in industrial wastewater and receiving waters, and also bioaccumulated in aquatic organisms at concentrations ranging from ng L^{-1} to µg L^{-1}.[3,17] The most frequently detected drugs include anti-inflammatories, analgesics, antidepressants, antibiotics, and lipid-lowering agents, all of which pose a risk to non-target species, potentially damaging both ecosystem function and human health.[18] Meeting these challenges will require an interdisciplinary approach combining nanotechnology, polymer chemistry and environmental science. Nanotechnology offers promising avenues for targeted remediation by enabling the design of the materials at the nanoscale, enhancing their capabilities for pollutant removal. Specifically, nanostructured materials can be engineered to selectively capture both organic contaminants and toxic heavy metals, providing a versatile and effective solution for environmental cleanup. In particular, nanoparticles offer a combination of high adsorption efficiency, stability and recoverability, as well as superior capacity and practical scalability.[19] Iron oxide nanoparticles (IONPs), particularly magnetite (Fe$_3$O$_4$), have garnered significant attention in this context owing to their magnetic nature and unique physicochemical characteristics, including high surface area and facile surface modification.[20–24] They have demonstrated high efficiency in water remediation, both in removing heavy metals (e.g. lead, mercury, and cadmium) and organic pollutants (e.g. dyes and pharmaceuticals).[20,25–27] Of particular interest are magnetic particles that exhibit superparamagnetic behaviour at room temperature. They display fully reversible magnetic behaviour with zero remanence and coercivity enabling easy manipulation via an external magnetic field while preventing particles' aggregation when the field is removed.[28] This property enables efficient contaminant removal by applying an external magnetic field, as well as easy recovery of the nanoparticles, improving their reusability and cost-effectiveness.[19,27] The selectivity and efficiency of IONPs can be further improved through tailored functionalisation. Effective strategies include introducing support materials, such as graphene, and using capping or stabilizing agents, such as cellulose, biopolymers or other green stabilizers, to enhance the stability of iron oxide nanoparticles (IONPs) and broaden their potential applications in environmental and biomedical fields.[21,23,29] In addition, advanced coating techniques such as atomic layer deposition (ALD), chemical vapor deposition (CVD), and layer-by-layer (LbL) assembly enable precise control over surface chemistry and thickness for enhanced material performance.[29] Commonly used stabilizers include phosphonic acids, carboxylic acids, dopamine, cysteine, trimethoxysilane, and amines.[30] To prevent aggregation, oxidation, and corrosion, and to increase the adsorption capacity of magnetic nanomaterials, these are typically coated with either organic layers (polymers or surfactants, such as polyethylene glycol and dextran) or inorganic elements (for instance, gold, platinum, cobalt oxide, aluminium oxide, silica, and activated carbon).[21,31–33] The use of polymers for coating is particularly important to improve colloidal stability under hydrophilic conditions and to protect the iron oxide core from degradation.[34,35] Within this context, poly (2-oxazoline)s, (POx), synthesised through the cationic ring-opening polymerization (CROP) of 2-oxazoline monomers, stand out for their exceptional versatility and tuneable chemistry.[36] Compared to the widely used poly(ethylene glycol) (PEG), POx not only maintain key attributes such as biocompatibility, low dispersity, and stealth properties but also offer superior stability, flexibility, and functionalization potential, making them a groundbreaking alternative in advanced material design.[37–43] In this paper, we aim to explore the synergistic potential of polyoxazoline-functionalised IONPs for the removal of pharmaceuticals and heavy metal ions from water. The customisable chemical structure of POx allows for the precise engineering of functional groups, while the predominantly hydrophilic nature of POx improves the compatibility of IONPs in aqueous media, thereby increasing their effectiveness in water treatment applications. The present work will describe in detail the synthesis, physicochemical characterization, and adsorption mechanisms, —examined through batch experiments—while outlining both prospects and challenges associated with this innovative technology. By harnessing the combined attributes of IONPs and polyoxazoline, this approach holds promise for addressing the persistent issue of pharmaceutical contamination in water resources, thereby contributing to environmental sustainability, and safeguarding public health.

Results and discussion

Synthesis and morpho-structural characterization

Fe$_3$O$_4$ nanoparticles were synthesized following the Radwan et al. co-precipitation technique, using FeCl$_3$·6H$_2$O and FeCl$_2$·4H$_2$O salts as starting materials.[21,44,45] Particles were then functionalized with two distinct poly(2-oxazoline)s, PAmOx and PiPOx, to enhance their performance for applications in water remediation.[46] PAmOx was selected for its aminic group, which enhances interactions with various

environmental contaminants, and PiPOx was chosen for its high hydrophilicity, making it suitable for water-based applications. Both polymers have already demonstrated potential in environmental remediation, further supporting their suitability for this purpose.[26] The synthesis of the polymers was carried out using a cationic ring-opening polymerisation technique.[47] The process starts with the use of methyl tosylate (**1**, Scheme S2, SI) as an initiator and the corresponding monomers (**2a** and **2b**, Scheme S2, SI). The ring-opening polymerisation technique is particularly valuable because it allows controlled growth of the polymer chain, ensuring a narrow molecular weight distribution and a well-defined structure. One of the key aspects of this synthesis is the introduction of a triethoxysilane group into the polymer chain. This functional group is critical for bonding the polymer to the iron oxide nanoparticles as it facilitates the attachment of the polymer *via* a silane coupling mechanism, which is known for its ability to form stable covalent bonds with metal oxide surfaces.[48,49] The triethoxysilane functionality was introduced using 3-aminopropyltriethoxysilane (APTES) as a terminating agent. In the ring-opening polymerisation of 2-oxazoline, the oxazolinium propagating end remains without decomposition after the monomer is consumed and is active to undergo nucleophilic attack by amine. Thus, (3-aminopropyl)triethoxysilane (**4**, Scheme S2 SI) was reacted with the oxazolinium (**3**, Scheme S2) to form the terminal group of the polyoxazoline (**5a** and **5b**, Scheme S2 SI). The morphology and size distribution of Fe_3O_4 nanoparticles were examined using transmission electron microscopy (TEM) and scanning electron microscopy (SEM). A small amount of diluted nanoparticle suspension in water was applied to the TEM grid and left to dry naturally before imaging. The nanoparticles were well-dispersed in the solution using sonication to ensure even distribution. The uncoated magnetic IONPs, shown in Fig. 1a,

exhibit a distribution of particles with varying sizes spread across the field of view. While some agglomeration is visible, individual nanoparticles remain distinguishable, with a mean core diameter of 11.9 ± 2.8 nm (Table S1, SI). The polyoxazoline-coated nanoparticles, on the other hand, display consistent spherical or quasi-spherical shapes with a uniform size distribution. Specifically, Fe_3O_4@PiPOx NPs have a size of 14.7 ± 1.3 nm (Fig. 1b), while those coated with PAmOx measure 14.2 ± 1.7 nm (Fig. 1c). As illustrated in Fig. 1b, Fe_3O_4@PiPOx forms tightly packed clusters, with the aggregation making it challenging to differentiate individual components due to their dense arrangement. In contrast, the Fe_3O_4@PAmOx nanoparticles appear less agglomerated, with clearer individual definition compared to the PiPOx-coated IONPs. This indicates that the polymer coating, particularly PAmOx, plays a significant role in stabilizing the nanoparticles and reducing agglomeration. The data obtained by TEM are consistent with the SEM results (Fig. 1d), confirming that the particles are predominantly spherical. SEM images further show that the hybrid particles retain a uniform spherical shape, with an average diameter of 15–20 nm (Fig. 1e and f), indicating that the surface modification does not significantly alter the overall shape of the nanoparticles. The size distribution of nanoparticles in aqueous solution was also assessed using Dynamic Light Scattering (DLS). The analysis shows relatively narrow distributions, with bare magnetite nanoparticles exhibiting a polydispersity index (PDI) of 0.394, while the polyoxazoline-coated particles had a lower PDI of 0.224 (Fe_3O_4@PAmOx) and 0.132 (Fe_3O_4@PiPOx), thus suggesting a more uniform particle size. DLS analysis (Table S1, SI) reveals a hydrodynamic diameter of 155.3 nm for the uncoated magnetite nanoparticles. Following the polyoxazoline coating, the hydrodynamic diameter increased to 169.7 nm for PiPOx (PDI 0.132) and decreased to 127.7 nm for PAmOx (PDI 0.224). These values,
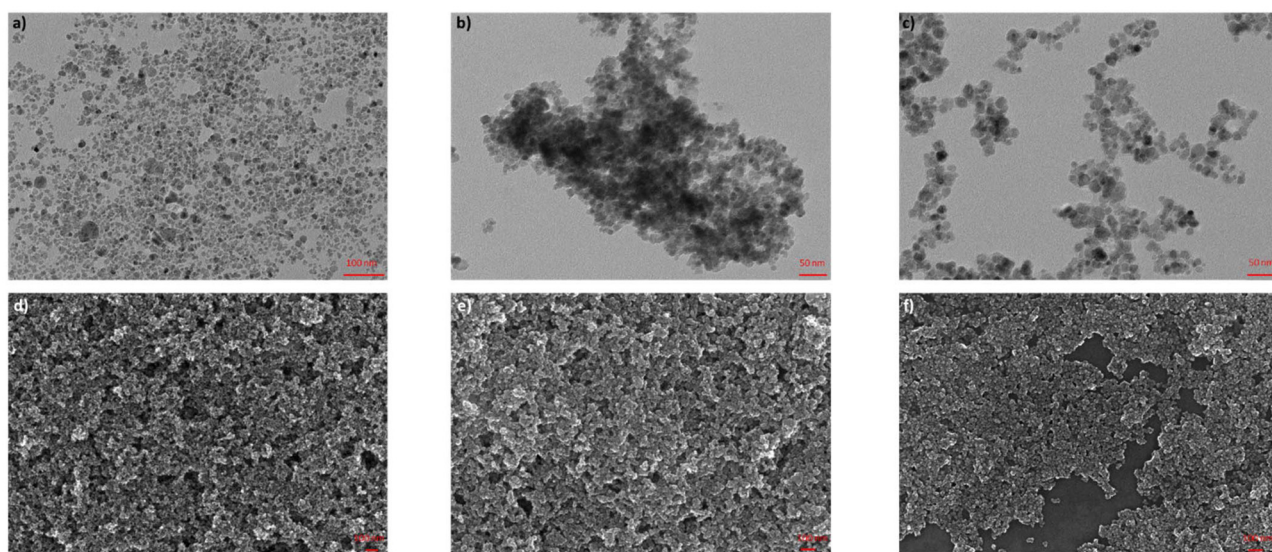

Fig. 1 TEM images of (a) bare IONPs, (b) Fe_3O_4@PiPOx and (c) Fe_3O_4@PAmOx; SEM images of (d) bare IONPs, (e) Fe_3O_4@PiPOx and (f) Fe_3O_4@PAmOx.

significantly larger than those obtained from TEM and SEM measurements, reflects DSL's sensitivity to solution-phase phenomena such as dynamic aggregation and agglomeration, which are not observable in images of dried samples. Additionally, DLS provides an indirect measures of particle size, relying on the frequency of particle movement in solution (Brownian motion), inherently differing from the direct imaging techniques of TEM and SEM. Therefore, discrepancies between hydrodynamic diameters determined by DLS and those obtained by microscopic methods are expected.

Molecular coating

Attenuated total reflectance (ATR) Fourier-Transform Infrared (FT-IR) spectroscopy was used to characterize the functional groups present in the nanoparticles. As they were thoroughly washed after synthesis, no mechanically deposited polymer was expected. Fig. 2a displays the ATR spectra of both bare and polyoxazoline-coated nanoparticles. The absorption band observed near 576 cm^{-1} confirms the presence of the Fe–O bond in the uncoated and functionalised IONPs.[50] After polyoxazoline functionalization, the emergence of new peaks in the 2800–3000 cm^{-1} region, attributed to C–H stretching vibration from aliphatic CH_2 and CH_3, provides unequivocal evidence of successful surface modification. Further supporting this, additional peaks are observed at 1635 cm^{-1} (Fe_3O_4@PAmOx) and 1651 cm^{-1} (Fe_3O_4@PiPOx), representing C=O stretching

vibrations, and at 1448 cm^{-1}, associated with N–H bending. The Si–O stretching vibration of APTES on the surface of Fe_3O_4 nanoparticles is assigned to the bands in the region between 1000 and 1100 cm^{-1}.[51] These spectroscopic data demonstrate successful polyoxazoline functionalization of the magnetite particles. Furthermore, UV-Vis spectrophotometry was performed on the dispersion of uncoated and polyoxazoline-functionalised iron oxide nanoparticles in distilled water. As revealed in Fig. 2b, all three samples exhibited the characteristic absorption peak of Fe_3O_4 at a wavelength of 275–301 nm.[52–54] Furthermore, the spectra of Fe_3O_4@PAmOx and Fe_3O_4@PiPOx clearly highlight the characteristic absorption peak of PAmOx and PiPOx, respectively, at approximately 210 nm, confirming the successful incorporation of polyoxazoline coatings. In addition, the thermogravimetric analysis (TGA) reveals distinct thermal decomposition profiles for the uncoated and polyoxazoline-coated iron oxide nanoparticles (Fig. 2c and d). Bare Fe_3O_4 nanoparticles exhibit a consistent weight loss of approximately 5% across the entire examined temperature range, attributed to the removal of physically and chemically adsorbed water.[55,56] In contrast, the polymer-functionalized samples exhibited significantly distinct weight loss patterns, directly reflecting the degree of polymer coating on the nanoparticle surface, and, consequently, providing insight into the magnetite content. Fe_3O_4@PAmOx shows a significant weight reduction of 52.88%, starting at around 200 °C, indicating a relatively thick polymer layer on the nanoparticles and its subsequent thermal decomposition. Conversely, Fe_3O_4@PiPOx displays a smaller weight loss of 19.97%, suggesting a thinner or less densely packed polymer coating. The decomposition in this sample began at a higher temperature, suggesting that the polymer in Fe_3O_4@PiPOx is more stable to thermal degradation. These differences in weight loss highlight variations in the extent of polymer coverage on the iron oxide nanoparticles, which influence their stability and functionalization efficiency. The grafting density calculations (number of polymer chains per unit surface area of the nanoparticles) further underscores this difference. Fe_3O_4@PAmOx displays a significantly higher grafting density (1.48 chains per nm) compared to Fe_3O_4@PiPOx (0.34 chains per nm), confirming more extensive polymer coverage in the former material. This disparity is likely due to the greater steric hindrance from the isopropyl group in PiPOx, limiting the number of polymer chains that can effectively bind to the nanoparticle surface. The grafting density was determined from TGA data by analysing the relative mass of the polymer and the residual mass of the Fe_3O_4 core at 500 °C. The number of polymer chains was then estimated by dividing the polymer mass by its molecular weight. The nanoparticle surface area was determined assuming spherical particles with radii measured from TEM data, while the number of particles was estimated from the nanomaterial mass.[57–59]

Fig. 2 (a) ATR spectra, (b) UV-Vis spectra, (c) TGA curves of bare Fe_3O_4 NPs (black), Fe_3O_4@PAmOx (red), and PAmOx (green); (d) TGA curves of bare Fe_3O_4 NPs (black), Fe_3O_4@PiPOx (blue), and PiPOx (green); (e) zeta potential (ζ) distribution; and (f) field-dependent magnetization loops (300 K) normalized to the particle weight.

Colloidal stability

The zeta potential (ζ) was evaluated to measure the colloidal stability and nanoparticle aggregation (Table S1 (SI) and Fig. 2f) in Milli-Q water at pH = 5.5. To ensure comprehensiveness, the analysis was extended across a pH range of 2 to 7,
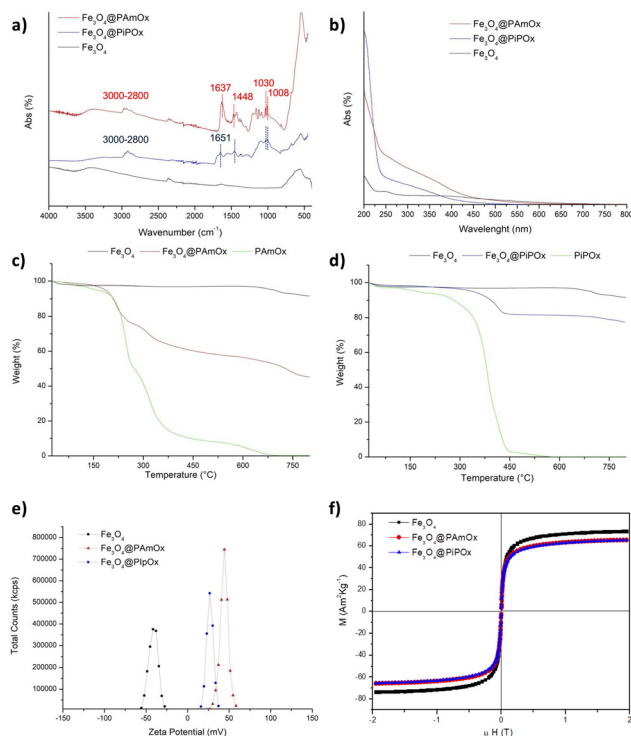
consistent with the conditions of the adsorption experiments. Importantly, no significant variations in the zeta potential were revealed (Fig. S5, SI). Low zeta potential values (0 to ± 5 mV) typically indicate enhanced van der Waals interparticle attractions, leading to rapid coagulation or flocculation. In contrast, a zeta potential value of around ± 30 mV generally reflects good nanoparticle stability, due to stronger electrostatic repulsive forces that prevent aggregation.[60] Maintaining nanoparticle stability is critical for consistent performance, particularly in applications such as water remediation. Given the marked differences in surface charge between bare and polymer-functionalised nanoparticles, zeta potential analysis was performed to confirm successful polymer coating. The uncoated Fe_3O_4 nanoparticles exhibit a negative zeta potential of -41.51 mV, indicating a highly charged surface. After coating with PiPOx and PAmOx, the surface charge becomes positive, with Fe_3O_4@PAmOx showing a stronger positive value (44.24 mV) compared to Fe_3O_4@PiPOx (16.67 mV). This shift suggests effective surface modification, with PAmOx providing greater stability or surface coverage than PiPOx. The fact that PAmOx plays an important role in stabilising the nanoparticles and reducing agglomeration in an aqueous system may be due to interactive stabilisation by the amine groups, which can form strong bonds with the nanoparticle surface. These interactive forces (hydrogen bonding, electrostatic interactions or even coordination with metal surfaces) can provide stronger stabilisation than steric stabilisation alone. These changes in surface charge may influence nanoparticle behaviour in suspension, including colloidal stability and interactions with biological environments.[61,62]

Magnetic properties

To investigate the influence of PAmOx and PiPOx coating on the magnetic properties of the Fe_3O_4 nanoparticles, field-dependent magnetization loops were performed at 300 K on bare and polyoxazoline-coated nanoparticles, as presented in Fig. 2e. All measurements were normalized by the effective content of the magnetic phase, determined from the TGA analysis. All samples exhibit superparamagnetic behavior,[63,64] with saturation magnetization (M_s) (Table S1, SI) closely matching the bulk value (~ 80 emu g^{-1}). The negligible difference in M_s values (within experimental error) suggests that the polyoxazoline functionalization does not significantly affect the intrinsic magnetic properties of the magnetic core.[46] This finding is particularly noteworthy because molecular coatings and its interactions with the nanoparticle surface are often reported to induce significant changes in saturation magnetization and magnetic anisotropy.[65] The persistence of the superparamagnetic behaviour after coating confirms that the nanoparticles remain magnetically responsive under low-strength external fields, enabling facile and rapid recovery from solutions, which is particularly advantageous in environmental applications due to tunable hydrophilicity.[7] The effectiveness of magnetic separation is demonstrated in Fig. 3, where the nanoparticles are collected using a cylindrical N52 Nd–Fe–B commercial permanent magnet.
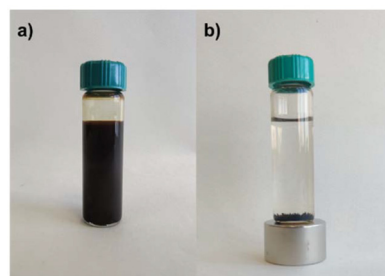

Fig. 3 Fe_3O_4@PAmOx nanoparticle solution: (a) before and (b) after the application of an external magnetic field.

Adsorption capability

The adsorption performance of Fe_3O_4@PiPOx and Fe_3O_4@PAmOx was evaluated by determining drug removal percentage and adsorption capacity (q_e). Considerable variations in performance were observed between the two materials for different drugs (Fig. 4). To compare the removal rates of the various pharmaceuticals, the same concentration was used for all of them, and the choice of 50 mg L^{-1} was related to the different solubilities of the drugs used in water. Table 1 and Fig. 5a present the recovery percentages and adsorption capacities (q_e, mg g^{-1}) for both Fe_3O_4@PiPOx and Fe_3O_4@PAmOx, across ten organic compounds. Recovery percentage quantifies how efficiently the nanoparticles capture drugs from a solution, while the adsorption capacity (q_e) measures the amount of drug adsorbed per gram of nanoparticles. For all the samples tested, performance in terms of both percent recovery and adsorption capacity, is higher for the composite material coated with PAmOx. For ibuprofen (7), Fe_3O_4@PAmOx shows almost twice the better performance (62.33% recovery, q_e of 31.61 mg g^{-1}) than Fe_3O_4@PiPOx (37.42% recovery, q_e of 18.98 mg g^{-1}). A similar trend was observed for indomethacin (8), for which Fe_3O_4@PAmOx

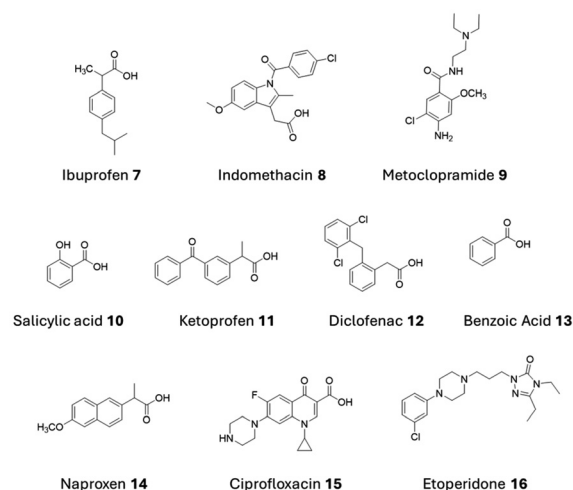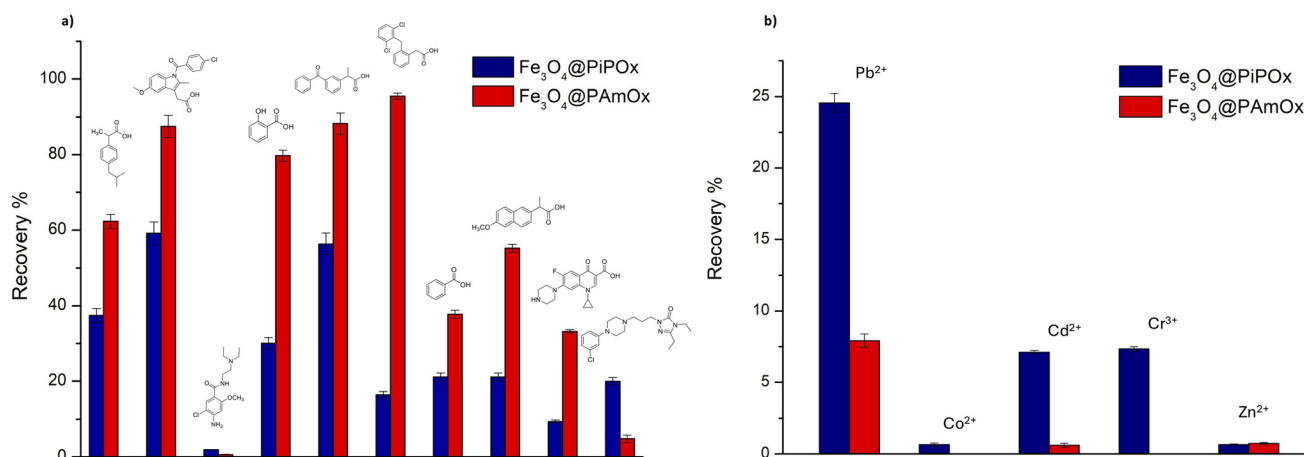**Fig. 4** Organic molecules used for the adsorption tests. Compounds **7**, **8**, **10**, **11**, **12**, **13**, **14**, and **15** have an acidic group.

Table 1 Percentage recoveries and adsorption capacities of each drug by Fe₃O₄@PiPOx and Fe₃O₄@PAmOx

	Recovery (%)		q_e (mg g^{-1})	
Drug	Fe₃O₄@PiPOx	Fe₃O₄@PAmOx	Fe₃O₄@PiPOx	Fe₃O₄@PAmOx
7	37.42	62.33	18.98	31.61
8	59.16	87.46	6.11	9.02
9	8.51	6.01	9.10	3.86
10	30.08	79.71	6.32	4.56
11	13.29	76.61	12.09	35.74
12	16.46	95.51	20.38	118.26
13	21.13	37.75	29.40	56.60
14	29.11	55.27	8.10	2.96
15	4.68	16.60	1.62	4.97
16	9.98	2.41	5.84	0.70

Fig. 5 Adsorption tests with (a) organic compounds and (b) heavy metal ions. The red bars correspond to the results obtained for Fe₃O₄@PAmOx and the blue bars for Fe₃O₄@PiPOx.

achieved 87.46% recovery and a q_e of 9.02 mg g^{-1} *versus* 59.16% recovery and 6.11 mg g^{-1} q_e for Fe₃O₄@PiPOx. The disparity is even more pronounced for diclofenac (**12**) with Fe₃O₄@PAmOx demonstrating a substantially higher adsorption capacity (118.26 mg g^{-1}) than Fe₃O₄@PiPOx (20.38 mg g^{-1}). Equally, benzoic acid (**13**) shows a q_e value of 56.60 mg g^{-1} for Fe₃O₄@PAmOx, while Fe₃O₄@PiPOx achieves a value of only 29.40 mg g^{-1}.

This enhanced performance of Fe₃O₄@PAmOx may be partly attributed to its denser surface polymer coverage, which would increase interactions with drug molecules. In addition, the superior performance of Fe₃O₄@PAmOx may be due to electrostatic interactions between the protonated amine groups of the polymer and drugs possessing carboxylate or other negatively charged groups. Conversely, Fe₃O₄@PiPOx exhibits lower adsorption efficiency. PiPOx, lacking functional groups that can act as bases, is likely to interact with drugs mainly through weak interactions, such as hydrophobic effects between the isopropyl moiety and the aromatic rings or aliphatic groups of the drugs. In addition, the isopropyl groups are likely to hinder the access of the largest and more structurally complex drugs to both the nanoparticle surface and the amidic groups characterizing polyoxazoline scaffolds. Overall,

the combination of increased surface coverage, favourable electrostatic interactions, and greater adsorption site accessibility makes Fe₃O₄@PAmOx a more efficient adsorbent compared to Fe₃O₄@PiPOx, particularly for acidic drugs. The adsorption of metal ions (Pb²⁺, Cd²⁺, Cr³⁺, Zn²⁺, and Co²⁺) by Fe₃O₄@PiPOx (blue bars) and Fe₃O₄@PAmOx (red bars) was also studied, and the results are presented in Fig. 5b and quantified in Table 2 (percentage recoveries and adsorption capacities). The adsorption experiment was carried out at an acidic pH because at alkaline pH values (above 7.0) metal hydroxide precipitation becomes prominent, depending on the nature and solubility of the metal.[66] Fe₃O₄@PiPOx exhibits high-grade Pb²⁺ recovery (>25%) compared to Fe₃O₄@PAmOx (approximately 5%). Even though a 25% Pb²⁺ removal rate seems modest compared to >80% by high-capacity adsorbents, it remains valuable for reducing ecological risk and enabling effective multi-stage treatment.[1] Enhanced recovery is also observed for Cd²⁺ and Cr³⁺ with Fe₃O₄@PiPOx (around 5–10%), although at lower levels than for Pb²⁺. Negligible adsorption of Zn²⁺ and Co²⁺ was observed for both materials. The contrasting performance of Fe₃O₄@PiPOx and Fe₃O₄@PAmOx under acidic conditions could be attributed to the differing nature of their side chains. Specifically, protona-

Table 2 Percentage recoveries and adsorption capacities of each heavy metal ion by Fe$_3$O$_4$@PiPOx and Fe$_3$O$_4$@PAmOx

Metal ions	Recovery (%)		q_e (mg g^{-1})	
	Fe$_3$O$_4$@PiPOx	Fe$_3$O$_4$@PAmOx	Fe$_3$O$_4$@PiPOx	Fe$_3$O$_4$@PAmOx
Pb^{2+}	24.56	7.92	24.85	7.54
Co^{2+}	0.66	—	0.66	—
Cd^{2+}	7.11	0.61	6.76	0.51
Cr^{3+}	7.34	—	7.14	—
Zn^{2+}	0.76	0.74	0.70	0.72

tion of the hydrophobic isobutyl side chains of PiPOx enhance its affinity for heavy metal ions, while the amine groups in PAmOx become protonated under acidic conditions, leading to electrostatic repulsion with metal cations and, thereby, reducing the adsorption capacity. In addition, these protonated amines can strongly attract water molecules, further hindering access to the blocking binding sites and limiting metal ion interaction. In contrast, the hydrophobic PiPOx side chains remain uncharged and do not attract water molecules, maintaining accessible binding sites and minimizing competition for protons, thus facilitating better adsorption of metal ions.

Materials and methods

Section S1 provides full details of materials, chemicals and instrumentation used.

Polymerization reactions

A two-neck round bottom flask equipped with an efficient reflux condenser and a magnetic stirring bar was charged with AmOx (20 mmol) and anhydrous ACN (12 mL). The system was kept under an argon atmosphere, 600 µL of a solution of 1 : 10 methyl tosylate : ACN was added, and the reaction mixtures was stirred for 48 h at 90 °C. After, the reaction was quenched by the addition of 10 eq. of the (3-aminopropyl)triethoxysilane (APTES) initiator solution in anhydrous ACN, and the resulting mixture was stirred for 2 h. Finally, the solvent was evaporated under vacuum and the residue was added to a solution of petroleum ether : diethyl ether (1 : 1). The polymer was recovered as a white precipitate, the supernatant was removed, and the product was washed twice with the petroleum ether : diethyl ether solution and dried *in vacuo*. GPC (*N,N* dimethylformamide (DMF) with LiBr (0.05 M)): M_n = 6.01 kDa, PDI = 1.11 for PBocOx; M_n = 3.08 kDa, PDI = 1.10 for PiPOx. PBocOx was deprotected by stirring the substate, dispersed in 5 mL of anhydrous DCM overnight after the addition of 500 µL of TFA. The solvent was removed using a rotatory evaporator and the final product PAmOx was precipitated by dropping the reaction solution into hexane/diethyl ether (v/v: 4/1), collected by centrifugation, and dried *in vacuo*. GPC (*N,N* dimethylformamide (DMF) with LiBr (0.05 M)): M_n = 3.03 kDa, PDI = 1.11.

Preparation of iron oxide nanoparticles

Radwan *et al.* employed the co-precipitation technique to prepare Fe$_3$O$_4$ nanoparticles using. FeCl$_3$·6H$_2$O and FeCl$_2$·4H$_2$O salts as a starting material.[21,44,45] The possible reaction in this process is shown as follows. Initially, a mixture containing both FeCl$_3$ and FeCl$_2$ was added to distilled water. Then this mixture of FeCl$_2$·4H$_2$O and FeCl$_3$·6H$_2$O mixed into one solution, and NH$_4$OH 25% (v/v) was added to the solution dropwise with vigorous stirring and mechanical agitation at a rate of 0.5 mL per second. After that, a dark-black precipitate resulted immediately. The solution was decanted and the obtained Fe$_3$O$_4$ sample was washed with distilled water several times, then washed with acetone and a drying operation was done in a furnace for five hours at 80 °C.

Preparation of the adsorbent materials (Fe$_3$O$_4$@PiPOx and Fe$_3$O$_4$@PAmOx)

A two-neck round bottom flask equipped with an efficient reflux condenser and a magnetic stirring bar was charged with APTES terminated-PAmOx or PiPOx (200 mg), 50 mg of IONPs, and anhydrous EtOH (6 mL). The system was sonicated for 1 h, then placed in an oil bath at 60 °C and stirred overnight. The functionalised nanoparticles were then washed with EtOH and H$_2$O several times to remove the free polymer.

Pharmaceutical adsorption

For batch binding studies, 10 mg of dry Fe$_3$O$_4$@PiPOx or Fe$_3$O$_4$@PAmOx particles were placed in 6 mL screw-capped plastic tubes and incubated with 4 mL of the aqueous solution of the pharmaceutical (50 mg L^{-1}). All the tubes were sealed and shaken in a thermostatic shaker (60 rpm) at 25 °C for 24 h. After incubation, the supernatant was removed, filtered with a 0.22 µm PTFE filter, and analysed by HPLC-UV to determine the remaining concentration of the pharmaceutical. All the adsorption experiments were conducted in triplicates.

Metal ion adsorption

To attain a cation concentration of 50 ppm, separately, an appropriate amount of the corresponding chloride salts (PbCl$_2$, CrCl$_3$, CdCl$_2$, CoCl$_2$, and ZnCl$_2$) was weighed and transferred in a plastic volumetric flask, then 0.01 M HCl in Milli-Q-grade water was added. After complete dissolution of salt, the solution was equilibrated at 25 °C and employed in adsorption experiments. In general, the polyoxazoline-functionalized magnetic nanoparticles (10 mg) were mixed with 5 mL of the

corresponding aqueous solution of metal ions for 24 h on a shaker to reach the adsorption equilibrium. After a defined time, the heavy metal solution was retrieved and filtered using a 0.22 μm PTFE filter. After acidification of the resulting solution with nitric acid 0.5%, concentrations were determined using inductively coupled plasma optical emission spectroscopy (ICP-OES). All the adsorption experiments have been conducted in triplicates.

Conclusions

The present study introduces a novel and innovative paradigm to water remediation, effectively leveraging the synergistic combination of Fe_3O_4 nanoparticles and poly(2-oxazoline) coatings. This approach provides a compelling avenue for mitigating the escalating challenge of water contamination. The study describes in detail the synthesis, preparation, and comprehensive characterization of Fe_3O_4 magnetic nanoparticles functionalized with two distinct poly(2-oxazoline) polymers: PiPOx and PAmOx, revealing their unique and complementary capabilities. Our experimental findings confirm the successful functionalization of the magnetic nanoparticles, wherein the differing poly(2-oxazoline) coatings exerted a marked influence on their stability, dispersibility, and surface charge, thereby affecting their overall performance in aqueous systems. Significantly, on the other hand, the magnetic properties of the core Fe_3O_4 nanoparticles remain largely unaltered compared to those of bare particles, ensuring efficient contaminant removal, facile particle recovery, and enhanced reusability under the application of an external magnetic field. The adsorption capabilities of both functionalized nanoparticles were evaluated against a range of commonly used pharmaceuticals and heavy metal ions, the two major classes of water contaminants. Fe_3O_4@PAmOx exhibits a superior adsorption capacity for acidic pharmaceuticals, a phenomenon that may be attributed to the favourable electrostatic interactions between the positively charged amine groups of the polymer and the negatively charged carboxylate groups of the target molecules. This enhanced adsorption performance is further ascribable to the higher grafting density of the polymer on the nanoparticle surface, which indicates more extensive surface coverage and, therefore, a greater number of active sites available for binding. Conversely, Fe_3O_4@PiPOx demonstrates a notable affinity for Pb^{2+} ions, which is one of the most toxic heavy metals commonly found in contaminated water sources. Moreover, the recovery values obtained are highly competitive with those of the established adsorbents described in the literature, including carbon-based materials and metal–organic frameworks (MOFs).[67–69] These distinct selectivity profiles – achieved *via* judicious selection of poly (2-oxazoline) – underscore the potential of tailored hybrid nanomaterials in addressing complex, multi-contaminant scenarios. By capitalising on the dual capabilities of Fe_3O_4@PiPOx and Fe_3O_4@PAmOx to selectively adsorb

pharmaceutical residues and heavy metal ions with the preserved magnetic properties of the core, this approach offers a versatile and efficient platform for advanced water purification. Their modular design allows for targeted pollutant removal, paving the way for scalable and sustainable water treatment technologies. Future research efforts will concentrate on several key areas such long-term performance and reusability of these materials under a variety of environmental conditions. Lastly, we aim to translate these findings from the laboratory to pilot-scale studies, assessing the feasibility of deploying these materials in real-world water treatment applications, such as treatment plants and point-of-use filtration devices. The tunability and adaptability of these materials to different environmental problems make our hybrid system promising for practical and scalable water purification.

Author contributions

Agnese Ricci: conceptualization, data curation, investigation, resources, methodology and writing – original draft; Luca Stefanuto: data curation, investigation, resources and writing – original draft; Sara Del Galdo and Barbara Capone: funding acquisition and writing – review and editing; Simone Pepi and Claudio Rossi: formal analysis; Valerio Graziani and Luca Tortora: formal analysis; Stefano Casciardi: formal analysis; Sawssen Slimani, Gaspare Varvaro and Davide Peddis: formal analysis and writing – review and editing; Daniela Tofani: writing – review and editing; Giancarlo Masci: validation, supervision and writing – review and editing; Tecla Gasperi: funding acquisition, resources, project administration supervision and writing – review and editing.

Conflicts of interest

There are no conflicts to declare.

Data availability

The primary study is supported by comprehensive experimental protocols and characterisation data in the Supplementary Information. It contains the synthesis of the iPOx and BocOx monomers, along with their ^{1}H NMR spectra, as well as those of the corresponding polymers, PiPOx and PBocOx. The synthesis plan for FeO_4-based nanoparticles functionalized with these polymers is also presented in the document. To verify structural and surface characteristics, characterisation methods like zeta potential measurements, XRD, and NMR are used. The study's conclusions are further supported by information on pH-dependent behaviour, nanoparticle reusability, and calibration curves for organic compounds. See DOI: **https://doi.org/10.1039/d5nr02457a**.

Acknowledgements

References

1 Z. Amini, M. Hatami-manesh, J. Aazami and M. Savabieasfahani, Ecological risk assessment of heavy metals (Pb, Cd, Cr, Ni, Zn, Fe) and metalloid (As) in surface sediment of Anzali International Wetland, Iran, *Geol. Ecol. Landsc.*, 2024, 1–19.

2 L. Lin, H. Yang and X. Xu, Effects of Water Pollution on Human Health and Disease Heterogeneity: A Review, *Front. Environ. Sci.*, 2022, **10**, 880246.

3 M. Zhai, B. Fu, Y. Zhai, W. Wang, A. Maroney, A. A. Keller, H. Wang and J.-M. Chovelon, Simultaneous removal of pharmaceuticals and heavy metals from aqueous phase via adsorptive strategy: A critical review, *Water Res.*, 2023, **236**, 119924.

4 S. Mitra, A. J. Chakraborty, A. M. Tareq, T. B. Emran, F. Nainu, A. Khusro, A. M. Idris, M. U. Khandaker, H. Osman, F. A. Alhumaydhi and J. Simal-Gandara, Impact of heavy metals on the environment and human health: Novel therapeutic insights to counter the toxicity, *J. King Saud Univ., Sci.*, 2022, **34**, 101865.

5 J. Briffa, E. Sinagra and R. Blundell, Heavy metal pollution in the environment and their toxicological effects on humans, *Heliyon*, 2020, **6**, e04691.

6 I. Karume, S. Bbumba, M. Kigozi, A. Nabatanzi, I. Z. T. Mukasa and S. Yiga, One-pot removal of pharmaceuticals and toxic heavy metals from water using xerogel-immobilized quartz/banana peels-activated carbon, *Green Chem. Lett. Rev.*, 2023, **16**, 2238726.

7 A. Shahzad, B. Aslibeiki, S. Slimani, S. Ghosh, M. Vocciante, M. Grotti, A. Comite, D. Peddis and

8 T. Sarkar, Magnetic nanocomposite for lead(II) removal from water, *Sci. Rep.*, 2024, **14**, 17674.

8 M. Balali-Mood, K. Naseri, Z. Tahergorabi, M. R. Khazdair and M. Sadeghi, Toxic Mechanisms of Five Heavy Metals: Mercury, Lead, Chromium, Cadmium, and Arsenic, *Front. Pharmacol.*, 2021, **12**, 643972.

9 Z. Fu and S. Xi, The effects of heavy metals on human metabolism, *Toxicol. Mech. Methods*, 2020, **30**, 167–176.

10 M. M. Jones, J. E. Schoenheit and A. D. Weaver, Pretreatment and heavy metal LD50 values, *Toxicol. Appl. Pharmacol.*, 1979, **49**, 41–44.

11 S. Lan, N. Amaeze, H. Obanya and C. Okoroafor, Occurrence of selected pharmaceuticals in industrial wastewater, receiving waters and fish, *Afr. J. Aquat. Sci.*, 2019, **44**, 401–408.

12 J. Kathuria, J. Kaur, N. J. Babu and M. Arora, Water remediation for pharmaceutical and personal care products (PPCPs) with metal organic frameworks: A review, *Results Chem.*, 2023, **6**, 101223.

13 A. H. A. Khan and R. Barros, Pharmaceuticals in Water: Risks to Aquatic Life and Remediation Strategies, *Hydrobiologica*, 2023, **2**, 395–409.

14 K. Samal, S. Mahapatra and M. Hibzur Ali, Pharmaceutical wastewater as Emerging Contaminants (EC): Treatment technologies, impact on environment and human health, *Energy Nexus*, 2022, **6**, 100076.

15 M. Desai, A. Njoku and L. Nimo-Sefah, Comparing Environmental Policies to Reduce Pharmaceutical Pollution and Address Disparities, *Int. J. Environ. Res. Public Health*, 2022, **19**, 8292.

16 H. Aib, M. S. Parvez and H. M. Czédli, Pharmaceuticals and Microplastics in Aquatic Environments: A Comprehensive Review of Pathways and Distribution, Toxicological and Ecological Effects, *Int. J. Environ. Res. Public Health*, 2025, **22**, 799.

17 J. Fick, H. Söderström, R. H. Lindberg, C. Phan, M. Tysklind and D. G. J. Larsson, Contamination of surface, ground, and drinking water from pharmaceutical production, *Environ. Toxicol. Chem.*, 2009, **28**, 2522–2527.

18 J. P. Fernandes, C. M. R. Almeida, M. A. Salgado, M. F. Carvalho and A. P. Mucha, Pharmaceutical Compounds in Aquatic Environments—Occurrence, Fate and Bioremediation Prospective, *Toxics*, 2021, **9**, 257.

19 Z. Qu, R. Leng and S. Wang, Nanomaterials Derived from Metal–Organic Frameworks and Their Applications for Pollutants Removal, *Rev. Environ. Contam.*, 2024, **262**, 12.

20 S. Nizamuddin, M. T. H. Siddiqui, N. M. Mubarak, H. A. Baloch, E. C. Abdullah, S. A. Mazari, G. J. Griffin, M. P. Srinivasan and A. Tanksale, *Nanoscale Mater. Water Purif.*, 2019, **17**, 447–472.

21 T. A. Aragaw, F. M. Bogale and B. A. Aragaw, Iron-based nanoparticles in wastewater treatment: A review on synthesis methods, applications, and removal mechanisms, *J. Saudi Chem. Soc.*, 2021, **25**, 101280.

22 M. Mohapatra and S. Anand, Synthesis and applications of nano-structured iron oxides/hydroxides – a review, *Int. J. Eng. Sci.*, 2010, **2**, 127–146.

23 P. Xu, G. M. Zeng, D. L. Huang, C. L. Feng, S. Hu, M. H. Zhao, C. Lai, Z. Wei, C. Huang, G. X. Xie and Z. F. Liu, Use of iron oxide nanomaterials in wastewater treatment: A review, *Sci. Total Environ.*, 2012, **424**, 1–10.

24 A. Ali, H. Zafar, M. Zia, I. Ul Haq, A. R. Phull, J. S. Ali and A. Hussain, Synthesis, characterization, applications, and challenges of iron oxide nanoparticles, *Nanotechnol., Sci. Appl.*, 2016, **9**, 49–67.

25 P. Patil, V. Mohite, K. Virani, P. Sarvalkar and N. Prasad, Adsorption of Heavy Metal Ions from Water Using Iron Oxide Nanoadsorbents: A Review of the Recent Literature, *J. Shivaji Univ. Sci. & Tech.*, 2023, **44**, 09–24.

26 E. Roma, P. Corsi, M. Willinger, N. S. Leitner, R. Zirbs, E. Reimhult, B. Capone and T. Gasperi, Theoretical and Experimental Design of Heavy Metal-Mopping Magnetic Nanoparticles, *ACS Appl. Mater. Interfaces*, 2021, **13**, 1386–1397.

27 P. P. Falciglia, E. Gagliano, P. Scandura, C. Bianco, T. Tosco, R. Sethi, G. Varvaro, E. Agostinelli, C. Bongiorno, A. Russo, S. Romano, G. Malandrino, P. Roccaro and F. G. A. Vagliasindi, Physico-magnetic properties and dynamics of magnetite (Fe3O4) nanoparticles (MNPs) under the effect of permanent magnetic fields in contaminated water treatment applications, *Sep. Purif. Technol.*, 2022, **296**, 121342.

28 J. L. Dormann, D. Fiorani and E. Tronc, *Adv. Chem. Phys.*, 1997, **650**, 283–494.

29 X.-M. Chen, H.-Y. Li, C.-C. Wei, J. Cheng, J. Diao, B. Xie and F. Pan, Selective Chemical Etching of Vanadium Slag Enables Highly Efficient and Clean Extraction of Vanadium, *ACS Sustainable Chem. Eng.*, 2025, **13**, 1327–1335.

30 W. K. Biftu, K. Ravindhranath and M. Ramamoorty, New research trends in the processing and applications of iron-based nanoparticles as adsorbents in water remediation methods, *Nanotechnol. Environ. Eng.*, 2020, **5**, 12.

31 C. Olariu, H. Yiu, L. Bouffier, T. Nedjadi, E. Costello, S. Williams, C. Halloran and M. Rosseinsky, Multifunctional Fe3O4 nanoparticles for targeted bi-modal imaging of pancreatic cancer, *J. Mater. Chem.*, 2011, **21**, 12650–12659.

32 N. Zhu, H. Ji, P. Yu, J. Niu, M. Farooq, M. Akram, I. Udego, H. Li and X. Niu, Surface Modification of Magnetic Iron Oxide Nanoparticles, *Nanomaterials*, 2018, **8**, 810.

33 Z. Karimi, L. Karimi and H. Shokrollahi, Nano-magnetic particles used in biomedicine: Core and coating materials, *Mater. Sci. Eng., C*, 2013, **33**, 2465–2475.

34 M. Barrow, A. Taylor, P. Murray, M. J. Rosseinsky and D. J. Adams, Design considerations for the synthesis of polymer coated iron oxide nanoparticles for stem cell labelling and tracking using MRI, *Chem. Soc. Rev.*, 2015, **44**, 6733–6748.

35 I. Ali, C. Peng, I. Naz and M. A. Amjed, Water Purification Using Magnetic Nanomaterials: An Overview, *Magn. Nanostruct.: Environ. Agric. Appl.*, 2019, 161–179.

36 M. Glassner, M. Vergaelen and R. Hoogenboom, Poly(2-oxazoline)s: A comprehensive overview of polymer struc-

tures and their physical properties, *Polym. Int.*, 2018, **67**, 32–45.

37 N. Adams and U. S. Schubert, Poly(2-oxazolines) in biological and biomedical application contexts, *Adv. Drug Delivery Rev.*, 2007, **59**, 1504–1520.

38 V. R. de la Rosa, A. V. Den Bulcke and R. Hoogenboom, Poly(2-Oxazoline)s: The Versatile Polymer Platform for Biomedicine, *Mater. Matters*, 2016, **11**, 3.

39 P. Venturini, S. Fleutot, F. Cleymand, T. Hauet, J. Dupin, J. Ghanbaja, H. Martinez, J. Robin and V. Lapinte, Facile One-Step Synthesis of Polyoxazoline–Coated Iron Oxide Nanoparticles, *ChemistrySelect*, 2018, **3**, 11898–11901.

40 S. Kurzhals, N. Gal, R. Zirbs and E. Reimhult, Controlled aggregation and cell uptake of thermoresponsive polyoxazoline-grafted superparamagnetic iron oxide nanoparticles, *Nanoscale*, 2017, **9**, 2793–2805.

41 L. Stefanuto, A. Ricci, E. Fardelli, S. Del Galdo, S. Pepi, V. Graziani, L. Tortora, C. Rossi, V. Arena, C. Bongiorno, E. Smecca, G. Capellini, B. Capone, D. Tofani and T. Gasperi, Engineering GO-pAmOx: A Polyoxazoline-Functionalized Graphene Oxide Composite for Selective Removal of NSAIDs and Organic Pollutants from Water, *ACS Omega*, 2025, **10**, 30087–30099.

42 A. Ricci, L. Stefanuto, S. Del Galdo, E. Fardelli, S. Pepi, S. Casciardi, B. Capone, C. Rossi, D. Tofani, G. Capellini, G. Iucci, G. Masci and T. Gasperi, Molecularly Imprinted Poly(2-(3-(amino)propyl)-2-oxazoline) for the Selective Removal of Ibuprofen from Aqueous Solutions, *ACS Appl. Polym. Mater.*, 2025, **7**(1), 42–53.

43 L. Stefanuto, A. Ricci, S. Del Galdo, C. Rossi, S. Pepi, E. Giordano, B. Capone, D. Tofani and T. Gasperi, 2-Oxazoline-Based Polymer for Pharmaceutical Products Adsorption in Aqueous Media, *J. Polym. Sci.*, 2024, **62**, 5656–5664.

44 M. A. Radwan, M. A. Rashad, M. Sadek and H. El-Azab, Synthesis, characterization and selected application of chitosan-coated magnetic iron oxide nanoparticles, *J. Chem. Technol. Metall.*, 2019, **54**, 303–310.

45 M. Namdeo, Magnetite Nanoparticles as Effective Adsorbent for Water Purification-A Review, Advances, *Recycl. Waste Manag.*, 2018, **2**, 1000135.

46 M. Abdolrahimi, M. Vasilakaki, S. Slimani, N. Ntallis, G. Varvaro, S. Laureti, C. Meneghini, K. N. Trohidou, D. Fiorani and D. Peddis, Magnetism of Nanoparticles: Effect of the Organic Coating, *Nanomaterials*, 2021, **11**, 1787.

47 S. Del Galdo, C. A. De Filippo, L. Stefanuto, S. Sennato, T. Gasperi, E. Chiessi and B. Capone, On the nature of the thermoresponsiveness of poly(2-isopropyl-2-oxazoline) in aqueous solution, *J. Mol. Liq.*, 2023, **392**, 123420.

48 G. Bissadi and R. Weberskirch, Formation of Polyoxazoline-Silica Nanoparticles via the Surface-Initiated Cationic Polymerization of 2-Methyl-2-oxazoline, *Polym. Chem.*, 2016, **7**, 5157–5168.

49 Y. Chujo, E. Ihara, S. Kure and T. Saegusa, Synthesis of triethoxysilyl-terminated polyoxazolines and their cohydro-

lysis polymerization with tetraethoxysilane, *Macromolecules*, 1993, **26**, 5681–5686.

50 S. Kumar, A. Balouch, E. Alveroglu, M. Jagirani, A. M. Moghal and D. Mal, Fabrication of nickel-tagged magnetic imprinted polymeric network for the selective extraction of Ni(II) from the real aqueous samples, *Environ. Sci. Pollut. Res. Int.*, 2021, **29**, 40022–40034.

51 A. Bordbar, A. Rastegari, R. Amiri, E. Ranjbakhsh, M. Abbasi and A. Khosropour, Characterization of Modified Magnetite Nanoparticles for Albumin Immobilization, *Biotechnol. Res. Int.*, 2014, **2014**, 705068.

52 O. Rahman, S. Mohapatra and S. Ahmad, Fe3O4 inverse spinal super paramagnetic nanoparticles, *Mater. Chem. Phys.*, 2012, **132**, 196–202.

53 M. Kumar, A. Sharma, I. Maurya, A. Thakur and S. Kumar, Synthesis of ultra small iron oxide and doped iron oxide nanostructures and their antimicrobial activities, *J. Taibah Univ. Sci.*, 2019, **13**, 280–285.

54 B. Abderrhmane, S. E. Laouini, A. Khelef, M. Tedjani and F. Guemari, Effect of Ferric Chloride Concentration on the Type of Magnetite (Fe 3 O 4) Nanoparticles Biosynthesized by Aqueous Leaves Extract of Artemisia and Assessment of Their Antioxidant Activities, *J. Cluster Sci.*, 2021, **32**, 1033–1041.

55 H. Fattahi, N. Arsalani and M. Nazarpoor, Synthesis and characterization of PVP-functionalized superparamagnetic Fe3O4 nanoparticles as an MRI contrast agent, *eXPRESS Polym. Lett.*, 2010, **4**, 329.

56 M. Ashraf, Z. Liu and W. Peng, Trisaminomethane–cobalt complex supported on Fe3O4 magnetic nanoparticles as an efficient recoverable nanocatalyst for oxidation of sulfides and C–S coupling reactions, *Appl. Organomet. Chem.*, 2020, **34**, 5260.

57 R. Zirbs, A. Lassenberger, I. Vonderhaid, S. Kurzhals and E. Reimhult, Melt-grafting for the synthesis of core–shell nanoparticles with ultra-high dispersant density, *Nanoscale*, 2015, **7**, 11216–11225.

58 D. N. Benoit, H. Zhu, M. H. Lilierose, R. A. Verm, N. Ali, A. N. Morrison, J. D. Fortner, C. Avendano and V. L. Colvin, Measuring the Grafting Density of Nanoparticles in Solution by Analytical Ultracentrifugation and Total Organic Carbon Analysis, *Anal. Chem.*, 2012, **84**, 9238–9245.

59 Y. Jiao and P. Akcora, Assembly of Polymer-Grafted Magnetic Nanoparticles in Polymer Melts, *Macromolecules*, 2012, **45**, 3463–3470.

60 Z. Németh, I. Csóka, R. Semnani Jazani, B. Sipos, H. Haspel, G. Kozma, Z. Kónya and D. G. Dobó, Quality by Design-Driven Zeta Potential Optimisation Study of Liposomes with Charge Imparting Membrane Additives, *Pharmaceutics*, 2022, **14**, 1798.

61 L. M. Al-Harbi and M. S. A. Darwish, Functionalized iron oxide nanoparticles: synthesis through ultrasonic-assisted co-precipitation and performance as hyperthermic agents for biomedical applications, *Heliyon*, 2022, **8**, e09654.

62 A. Kmita, D. Lachowicz, J. Żukrowski, M. Gajewska, W. Szczerba, J. Kuciakowski, S. Zapotoczny and M. Sikora, One-Step Synthesis of Long Term Stable Superparamagnetic Colloid of Zinc Ferrite Nanorods in Water, *Materials*, 2019, **12**, 1048.

63 G. Prabha and V. Raj, Preparation and characterization of chitosan-Polyethylene glycol-polyvinylpyrrolidone-coated superparamagnetic iron oxide nanoparticles as carrier system: Drug loading and in vitro drug release study, *J. Biomed. Mater. Res., Part B*, 2016, **104**, 808–816.

64 H. Esmaeili and S. Tamjidi, Ultrasonic-assisted synthesis of natural clay/Fe3O4/graphene oxide for enhance removal of Cr(VI) from aqueous media, *Environ. Sci. Pollut. Res. Int.*, 2020, **27**, 31652–31664.

65 S. Slimani, A. Talone, M. Abdolrahimi, P. Imperatori, G. Barucca, D. Fiorani and D. Peddis, Morpho-Structural and Magnetic Properties of CoFe2O4/SiO₂ Nanocomposites: The Effect of the Molecular Coating, *J. Phys. Chem. C*, 2023, **127**, 8840–8849.

66 A. S. Olawale, Biosorption of Heavy Metals from Aqueous Solutions: An Insight and Review, *Arch. Ind. Eng.*, 2020, **3**, 1–31.

67 S. Lin, Y. Zhao and Y. S. Yun, Highly Effective Removal of Nonsteroidal Anti-inflammatory Pharmaceuticals from Water by Zr(IV)-Based Metal-Organic Framework: Adsorption Performance and Mechanisms, *ACS Appl. Mater. Interfaces*, 2018, **10**, 28076–28085.

68 H. Hosney, M. ElShourbagy, A. Abdelrady, T. Wagner, E. Borén, M. Ahmed and P. N. Lens, Micropollutant removal from domestic wastewater effluent by softwood-biochar and sludge-biochar for safe reuse applications, *Water Reuse*, 2025, **15**, 90–108.

69 F. Zhao, S. Fang, Y. Gao and J. Bi, Removal of aqueous pharmaceuticals by magnetically functionalized Zr-MOFs: Adsorption Kinetics, Isotherms, and regeneration, *J. Colloid Interface Sci.*, 2022, **615**, 876–886.